Nationaal Lucht- en Ruimtevaartlaboratorium
National Aerospace Laboratory NLR

NLR-TP-97239

A new test facility for the study of interacting pressure waves and their reduction in tunnels for high speed trains

W.B. de Wolf and E.A.F.A. Demmenie

DOCUMENT CONTROL SHEET

	ORIGINATOR'S REF.		SECURITY CLASS.
	NLR TP 97239 U		Unclassified

ORIGINATOR
National Aerospace Laboratory NLR, Amsterdam, The Netherlands

TITLE
A new test facility for the study of interacting pressure waves and their reduction in tunnels for high speed trains

PRESENTED AT
the 9th International Conference on Aerodynamics and Ventilation of Vehicle Tunnels, 6-8 October 1997, Aosta Valley, Italy.

AUTHORS	DATE	pp	ref
W.B. de Wolf and E.A.F.A. Demmenie	970425	32	6

DESCRIPTORS

Compression waves	Scale models
Data acquisition	Test facilities
Gun launchers	Transfer tunnels
Performance prediction	User requirements
Rail transportation	

ABSTRACT
The National Aerospace Laboratory NLR in the Netherlands recently developed a test facility that provides duplication of the interacting pressure waves in railway tunnels on model scale at realistic conditions. In this facility it is possible to launch train models with a diameter of 20 mm and a length up to 2.5 meters (scale approximately 1 : 175) at velocities up to 500 km/hr.
After its launch, the train model is guided through a tunnel model of typically 20 cm^2 cross section and length of 10 meters. The tunnel model has a flexible layout, allowing easy variation of the cross section (tunnel blockage ratio) and entry configurations.
The pneumatic launch system, the guidance of the train model and measurement techniques will be described in detail and some test results will be shown.

Contents

20 Figures

(32 pages in total)

This page is intentionally left blank.

A NEW TEST FACILITY FOR THE STUDY OF INTERACTING PRESSURE WAVES AND THEIR REDUCTION IN TUNNELS FOR HIGH SPEED TRAINS.

By W.B. de Wolf and E.A.F.A. Demmenie
National Aerospace Laboratory NLR
The Netherlands

SYNOPSIS

The National Aerospace Laboratory NLR in the Netherlands recently developed a test facility that provides duplication of the interacting pressure waves in railway tunnels on model scale at realistic conditions. In this facility it is possible to launch train models with a diameter of 20 mm and a length up to 2.5 meters (scale approximately 1 : 175) at velocities up to 500 km/hr.

After its launch, the train model is guided through a tunnel model of typically 20 cm^2 cross section and length of 10 meters. The tunnel model has a flexible layout, allowing easy variation of the cross section (tunnel blockage ratio) and entry configurations.

The pneumatic launch system, the guidance of the train model and measurement techniques will be described in detail and some test results will be shown.

1 INTRODUCTION

When the nose and the tail of a train pass the entrance of a railway tunnel a compression and an expansion wave is generated. These waves propagate at nearly the speed of sound towards the tunnel exit, where they are reflected. A compression wave returns as an expansion wave and vice versa. This leads to a wave interference pattern in the tunnel, that will cause fast pressure variations on the train itself. The amplitude of these pressure variations increases with the square of the train speed and has become an important issue for high speed trains currently in operation and under development.

The Netherlands are certainly not a country with high hills and mountains that would require railway tunnels. However, for Dutch integration into Europe’s fast train network a new railway will be constructed that will use tunnels. For instance tunnels with a length of about 1.5 km will be used for passage under two rivers and one tunnel of about 9 km is planned to

minimize the environmental impact on the so-called green heart of Holland which should be preserved as a typically Dutch countryside.

It was desired to maintain the train speed during passage of these tunnels up to a value of 300 km/hr. Therefore the project team High Speed Line South (HSL-Zuid) working for the Dutch Railways (NS) considered a number of measures on the tunnel design to reduce the pressure variations inside. The effects of these measures were determined theoretically using the well known method developed by Vardy (see e.g. Ref. 1).

Considering the vast consequences of an unfavourable discrepancy between the theoretical predictions and the final outcome of pressure reducing measures, a second, independent prediction, preferably based on experiments on model scale, was deemed necessary by HSL. Since the National Aerospace Laboratory NLR was also involved in earlier aerodynamic research for NS, the NLR was approached to conduct a feasibility study for such an experimental verification.

This feasibility study led to a proposal for a test set-up supported by in-house activities to explore the experimental techniques to be employed. Some of these techniques were new to the NLR and their use had to be demonstrated before further commitments could be made.

The present paper will report on the development of the new techniques and the design considerations that have led to the final test facility that has become operational by the end of 1996. To demonstrate the capabilities of the new T3F (Train Tunnel Test Facility) some test results will be shown that were obtained before starting the actual contract work that was performed for HSL.

2 THE PROPAGATION OF COMPRESSION AND EXPANSION WAVES IN RAILWAY TUNNELS

Figure 1 shows what happens if a train of 400 m length travels at 300 km/hr (83.3 m/s) through a tunnel of 1500 m length. The events are depicted in a so-called wave diagram. In this diagram the horizontal axis represents the axial position in the tunnel and the vertical axis represents the time, elapsed since the head of the train entered the tunnel opening.

Above the wave diagram a few "snapshots" are given, depicting the position of the train and the compression (I) and expansion (II) waves in the tunnel at 2.5 second time intervals. Positions x_1 and x_2 in the tunnel are discussed later. In the wave diagram the position of the train is indicated by the shaded zone bounded by straight lines III and IV, indicating the head and tail of the train respectively. The head of the train arrives at the tunnel exit at t = 18.0 sec while the tail follows 4.8 sec later.

When the head of the train enters the tunnel, a pressure wave (line Ia) is generated that propagates into the tunnel ahead of the train. This pressure wave propagates at a speed, very close to the speed of sound of 1225 km/hr (340 m/s) and reaches the tunnel exit at t = 4.4 sec. For given atmospheric conditions (pressure and temperature) the amplitude of the pressure wave depends on the speed of the train and on the so-called blockage ratio β (defined as the train cross section area A_{train} divided by the tunnel cross section area A_{tun}). According to Sellmann (Ref.2) for a realistic blockage ratio of $\beta = 0.2$ and a train speed of 83.3 m/s the pressure immediately after the compression wave is 2.7 kPa higher than the initial atmospheric value of 103 kPa in the tunnel (at standard conditions).

In fact, the blockage ratio must include the so-called displacement area of the boundary layer that develops on the train. The result is that the initial blockage, corresponding with the head of the train entering the tunnel is followed by a gradual increase, followed by a sudden decrease when the tail of the train passes the tunnel entrance. The pressure waves that are generated at the tunnel entrance are then a fast pressure rise (from the head of the train) followed by a gradual pressure rise due to the increasing displacement thickness of the boundary layer on the train. This is followed by a fast pressure drop (from the tail of the train entering the tunnel). At some distance in the tunnel $x_2 > x_1$ (see figure 1) the complete wave system between Ia and IIa is ahead of the train. Figure 2 shows schematically the resulting pressure history as sensed by a transducer on the tunnel wall at x_2 = 600 m, until t = 7.2 sec (arrival of train nose at location x_2). From this pressure history it should in principle be possible to derive the aerodynamic shape of the train, including the displacement effect of the boundary layer. As such the pressure history between t = 1.8 and 6.6 sec is a somewhat distorted image of the aerodynamic cross section distribution along the length of the train.

Returning to figure 1, the steep expansion wave IIa starting at t = 4.8 seconds, when the tail of the train enters the tunnel, has reached the head of the train at t = 6.0 seconds. About one second later, at t = 7.1 second, the head of the train is hit by an other steep expansion wave. This wave Ib results from the reflection of the initial pressure wave Ia that reflects on the tunnel exit opening as an expansion wave of almost the same strength. This expansion Ib is followed by a sudden decrease of the pressure when the nose of the train arrives at 7.2 sec.

The expansion waves (line Ib and IIa) reflect as compression waves (line Ic and IIb) on the tunnel openings at t = 8.8 sec t = 9 sec respectively. As a result a complicated pattern of upstream and downstream compression and expansion waves is created in the tunnel that causes pressure variations on the train during the passage.

In case of a longer train (or a shorter tunnel) the meeting of both expansion waves (line Ib and IIa) will not be ahead of the train, as in figure 1, but at some location on the train itself. At 300 km/hr this occurs when the train is longer than 0.3 times the length of the tunnel. At 120 km/hr this critical train length is 0.16 times the tunnel length. Coincidence of both expansion waves on the train will lead to a very fast pressure variation (in the present case - 5.2 kPa in one step rather than in two steps), which may cause additional discomfort to the passengers.

It is remarked here that secondary reflections of compression and expansion waves on the train nose and tail were not included in the wave-diagram and this discussion.

3 FACILITY REQUIREMENTS

In the test facility, the wave diagram of figure 1 must be duplicated on a reduced time and length scale. This is the case if the following conditions are satisfied:

a) Duplication of the ratio of the train velocity V to the speed of sound a, which corresponds to duplication of the Mach number M = V/a.
b) Duplication of the train length to tunnel length ratio.

To reproduce the strength of the pressure waves, also a third condition must be met:

c) Duplication of the blockage ratio $\beta = A_{train}/A_{tunnel}$.

It is of interest to observe that the velocity must be taken to the full scale value (at room temperature) and is not subject to scaling. The wave diagram is based on a one-dimensional flow model where the pressure waves are assumed to be plane waves. Thus in principle, the length scale can be chosen independently of the diameter scale. However, near area discontinuities these waves will have a 3-dimensional character and therefore it was decided to apply the same scale for axial and cross dimensions.

With respect to size, train models as small as 20 mm diameter have been used successfully (Refs. 3, 4). With respect to costs, a small facility is to be preferred. On the other hand Reynolds effects cannot be ignored since friction forces tend to become relatively more important with decreasing dimensions.

A direct effect of the Reynolds number is on the attenuation of the pressure waves propagating in the tunnel. On the other hand this Reynolds effect is partially compensated by the higher roughness of a full scale tunnel and by using a smooth wall for the tunnel model. This can be concluded from the investigations by Matsuo et al. (Ref. 3). They give experimental data for the attenuation on model scale and full scale. For instance after 200 tunnel diameters the amplitude of a compression wave with a strength of 2.7 kPa has reduced to 96 percent in a full scale (rough) tunnel and to 90 percent in a smooth model scale tunnel (tube) with a hydraulic diameter of 23.6 mm (corresponding to so-called k factors of $2*10^{-4}$ and $5*10^{-4}$ respectively as derived from Ref. 3). Based on these findings and the larger hydraulic diameter (larger than 50 mm) chosen for the test facility (T3F), the resulting differences in attenuation between model and full scale were considered to be acceptable.

Apart from this direct Reynolds number effect on the strength of the pressure waves, an indirect effect exists. The boundary layer on a smooth model train is relatively thicker than on a smooth real train. As a result the pressure rise after the initial compression wave will therefore be higher on modelscale (higher effective blockage ratio). On the other hand the real train will have drag components like the pantograph that will not be present on the train model which will have a simple cylindrical shape and a faired nose and tail.

Based on the above considerations, a train model diameter of 20 mm was selected, resulting in a scale 1:175. Because a train length of 400 m full scale had to be considered as a standard test case, a corresponding train model length of 2.3 m results. A brief comment on the resulting scale effects related to the boundary layer on the train will follow when discussing some experimental results obtained in the new test facility.

With respect to the performance requirements, a train velocity of at least 300 km/hr (83.3 m/s) had to be achieved for the measurements for HSL. To increase its potential, the facility should be designed for a higher train velocity if this would not entail significantly higher costs. It was thought that a maximum velocity of 500 km/hr (139 m/s) would be an interesting design target, considering possible future applications like magnetic levitation trains.

4 CHOICE OF THE TYPE AND PRINCIPLES OF THE FACILITY

Experiments on compression waves propagating in ducts have a long tradition. The basic tool for these studies is the shock tube, schematically shown in figure 3. A shock tube essentially consists of a high pressure section (the driver) and a low pressure section (the driven part). Both sections are separated by a membrane. When this membrane is broken, a shock wave develops that propagates into the driven tube. The driven tube can be open to the atmosphere, simulating a train tunnel exit situation. In this way, the reflection of the compression wave on the open end and means to reduce their strength can be studied.

However, in this way the effect of the returning expansion wave on the moving train, let alone its interference with the expansion wave generated by the tail of the train cannot be studied. This requires a facility with a (model) train travelling through a tunnel. The velocity of this train must be equal to the full scale value, see chapter 3.

For the propulsion of the train model various principles can be applied. Known from the literature are the catapult (Ref. 6), gun powder (Ref. 3) and a pneumatic launcher (air gun) (Ref. 4). Velocities of 55 m/s have been attained with a catapult. Velocities above 300 m/s were reported using gun powder and with pneumatic drives velocities of 160 m/s were attained. All figures relate to train in tunnel experiments and are considered state of the art.

The design speed for the present application is at least 85 m/s and a catapult was not considered suitable. A gun powder drive will lead to very high peak accelerations and tailoring of the charge to various test conditions (train weight and launch velocity) will be more complicated than with a pneumatic drive. Also additional safety aspects play a role.

It was therefore decided that the facility should be based upon a pneumatic launch system (air gun). At NLR an air gun was available at the Structures and Materials Department. This air gun has been used for the launching of 25 gram projectiles at 80 m/s on aircraft structures to study impact damage on composites. Figures 4 and 5 show the set-up and some technical details. This formed the basis of exploratory tests on the development of the new T3F.

As shown in figure 5, the air gun has the same lay-out as the shock tube. The difference is that a projectile is added downstream of the membrane separating the driver and the driven section. The projectile has a sliding fit in the driven section, which now serves as a launch tube or (gun) barrel. The projectile and the launch tube have preferably a circular cross section. The membrane can be ruptured due to overpressure but a mechanical device is preferred to improve the repeatability.

5 EXPLORATORY TESTS

5.1 Provisional test set-up

Exploratory test were carried out to address three questions that had to be dealt with before embarking on a more permanent facility. These three questions were:

a) The effect of the blast wave and the air jet from the launch tube on the pressure in the test tunnel.
b) The feasibility of a long train model with a length to diameter ratio of about 100.
c) The guidance of the train through the test tunnel.

The original air gun depicted in figures 4 and 5 was used as a starting point. The driver volume was 4 litres and the launch tube had a diameter of 21 mm and a length of 1 meter. An available tube with 62 by 62 mm square cross section and 2.3 meters long was used as a provisional test tunnel. The distance between the tunnel entrance and the end of the launch tube was taken as 1.5 meters, a realistic starting point for investigations on the reduction of blast wave effects.

Three fast response transducers were mounted in the tunnel wall to measure the pressure variations caused by the pressure waves and the passage of the train. The train velocity was determined from the time that the light path to a photo electric cell was interrupted by the passing train model (of given length).

5.2 Blast wave and air jet effects from the launch tube

During its acceleration through the launch tube, pressure will build up ahead of the train and an air jet will flow from the opening of the launch tube. This jet may have effect on the pressure in the test tunnel downstream. When the tail of the train leaves the launch tube, a blast wave may develop when the residual back pressure in the launch tube is higher than atmospheric. This blast wave propagates as a spherical shock wave that will hit the test tunnel entrance and may affect the pressure inside. This blast wave is followed by a high velocity jet which may also affect the pressure in the test tunnel.

To demonstrate these effects, a test was performed with the original air gun depicted in figure 4, using a driver pressure of 4 bar. This results in a residual back pressure of 3.56 bar, leading to a supersonic jet from the opening of the launch tube. Figure 6 shows the pressure measured in the test tunnel at a position 0.3 meter from the tunnel exit. The upper half shows the pressure trace with a standard 25 gram projectile of about 25 mm length and the lower trace is the result without projectile at the same driver pressure of 4 bar. In both cases an initial pressure disturbance can be observed followed by a gradual increase in about 5 milliseconds to a level of about 2.3 kPa without projectile and 1.5 kPa with projectile.

The velocity of the projectile was about 80 m/s. The tunnel blockage ratio was 0.08 and should have resulted in a clearly visible compression wave in the order of 1.0 kPa (using Sellmann). However, in this case jet and blast wave effects from the launch tube are completely obscuring the pressure wave caused by the projectile.

The jet driven by the back pressure can be completely eliminated by reducing the residual back pressure to a sub-atmospheric value. The projectile launcher was therefore modified by reducing the driver volume to 0.2 litres and by increasing the length of the launch tube to 4 meters. In this case, the residual back pressure will remain below one atmosphere for driver pressures below 18 bar.

These modifications were implemented and a test was performed with 0.52 m long train model in a 2.5 m long tunnel with cross section of 40 mm by 40 mm (to increase the blockage ratio to a more realistic value of 0.2). A driver pressure of 8 bar was used, resulting in a train velocity of 71 m/s.

The effectiveness of the modifications is illustrated in figure 7 showing the pressure history measured half way the tunnel. The initial pressure disturbance has disappeared completely. The first pressure variation measured by the transducer is a step of 1.7 kPa due to the arrival of the first compression wave, generated when the nose of the train enters the tunnel. This amplitude compares well with a value of 1.9 kPa using the expression of Sellmann (Ref.2). The pressure step is followed by a gradual increase due to the train boundary layer as

discussed earlier.

The principle of a sub-atmospheric residual back pressure was adopted as a design requirement for the T3F. It is noted that in the experiment of figure 7 no provisions were taken to eliminate the air jet in front of the train model, but this jet had apparently no measurable effect at this train velocity. To avoid any problem at higher velocities an extra provision was made on the T3F to completely eliminate also the forming of an air jet ahead of the train in the launch tube (see section 7).

5.3 The train model and its guidance

The launch tube diameter of 21 mm resulted in the use of cylindrical train models with a slightly smaller diameter. To limit the model weight when using long train models, balsa wood was selected that is commercially available in 20 mm diameter stock. Its weight varies between 0.050 and 0.080 kg per meter length. To experimentally verify its strength and possibly its deformation in the launch tube, a series of tests were performed in the 4 meter long launch tube. The length of the train models was gradually increased from 0.2 meters to 1.5 meters and driver pressures of up to 8 bar were used without any problem.

In case of (these) longer train models a form of guidance had to be developed to prevent the model dropping below the tunnel opening or hitting the tunnel walls during a passage. The guidance should start at the end of the launch tube, bridge the empty space to the tunnel opening and extend along the full tunnel length. A three point guidance using nylon slide rails was considered, but problems of alignment, rail support and model wear were anticipated. Although it was thought that these problems could be solved, a novel and very simple guidance method was developed instead.

The method is depicted in figure 8. Two parallel piano wires are used that extend from the launch tube opening to beyond the exit of the test tunnel. A metal ring with two diametrically opposed eyelets can slide along these wires. The outer diameter of the ring is equal to the train diameter. The head of the train model had a small forward facing step, mated to the ring. Prior to the launch the ring is positioned at the exit of the launch tube. When the head of the train has reached the exit of the launch tube it picks up the ring and the combination continues its way, guided along the wires.

To provide a guidance to the rear end of the train, a second ring with an inner diameter, that is somewhat larger than the train diameter, can be used. This tail ring is connected to the first (nose) ring using thin ropes of a length slightly less than the train length. However it generates a small pressure disturbance and experience has shown that for many test conditions the second ring is not necessary.

6 DESIGN CALCULATIONS FOR THE LAUNCHER FOR THE NEW TRAIN TUNNEL TEST FACILITY T3F

According to the requirements a launch velocity of at least 300 km/hr (83.3 m/s) had to be attained. A higher velocity should be possible if this would not entail significantly higher costs. Presently no need is seen for a velocity higher than 500 km/hr (139 m/s). As stated in section 3, the train model diameter was specified as 20 mm and its length as 2.3 m.

For a given driver pressure, the initial acceleration of the train model is inversely proportional to its specific mass. A lower mass leads thus to a shorter launch tube and/or a lower driver pressure to reach the same model velocity. The average mass of a balsa wood train model with 20 mm diameter lies between 0.050 and 0.080 kg/m. Thus a 2.30 m long train model would have a mass between 0.115 and 0.185 kg. A reference mass of 0.160 kg was selected for the following design calculations.

The driver pressure should remain below the natural bursting limit of the membrane. Tests showed that for the mylar membrane material to be used, a driver pressure of 20 atm. should not be exceeded.

The residual back pressure should not exceed a value of 0.8 atm. At this residual pressure, no air jet will develop from the launch tube opening when the tail of the train leaves the launch tube, see section 5.2.

With these requirements and constraints, performance calculations were made to establish the length of the launch tube and the driver volume. A simple theoretical model was used.

If it is assumed that the pressure behind the train model (the back pressure) varies according to an adiabatic process and if the pressure in front of the train remains atmospheric, while neglecting wall friction, the acceleration (a) depends as follows on the position x of the tail of the train model in the launch tube:

$$a = \frac{dv}{dx} = \frac{p_d A}{m}\left[\left(\frac{Vol_d}{Vol_d + Ax}\right)^{1.4} - \frac{p_{atm}}{p_d}\right]$$

In this equation p_d is the driver pressure and p_{atm} is the atmospheric pressure [N/m^2], A is the cross section area of the launch tube [m^2], Vol_d is the driver volume [m^3] and m is the mass of the train model [kg].

This equation can be integrated numerically for a series of p_d, Vol_d, A and m combinations. The integration is stopped when the back pressure has reached a value of 0.8 p_{atm}. This conservative value is chosen rather than 1.0 p_{atm} because in practice the (local) back pressure can be higher than assumed (average) value in the model (reflected waves in the tube behind the model).

As a result, figure 9 shows the launch velocity as a function of the tube length for different values of the driver pressure. The corresponding driver volumes (required for a residual (back) pressure of 0.8 atm) are indicated with dotted lines. The results show that a velocity of 300 km/hr can be attained with a launch tube length of about 6.5 meters and a driver pressure of 20 atm. to be combined with a driver volume of 0.25 litres. With the same driver pressure, 500 km/hr is possible with a launch tube length of 20 meters and a driver volume of 0.75 litres.

After performing a trade-off study and considering that in many cases a train model with less mass can be employed (shorter length or lower specific weight), the length of the launch tube was set at L = 15 meters. This point is indicated in figure 9 and should allow a maximum velocity of about 120 m/s (420 km/hr) for the reference train model. The driver pressure is then about 17 atm. and the driver volume 0.67 litre.

Figure 10 shows the launch velocity as function of the driver pressure for the selected length L = 15 m and Vol_d = 0.67 litres. The reference mass (0.160 kg) is used but also the performance for other train model masses are shown. It is noted that for a given driver pressure the velocity increases inversely proportional to the square of the model mass (kinetic energy remains the same). It is shown that a maximum velocity of 500 km/hr (139 m/s) should be obtainable on the basis of the assumptions in the theoretical model when using a train model weight of approximately 0.120 kg.

When the facility is operated at lower driver pressures, the back pressure reaches the atmospheric value well before the tail of the train reaches the end of the launch tube. At that point the acceleration is zero and the train model has reached its highest velocity in the launch tube. Beyond that point the train model starts to decelerate. This is illustrated in figure 11, which shows the velocity of the train model as a function of the position of its tail in the launch tube. When the driver pressure is lower than 5.35 atm. the tail of the train model will not leave the launch tube and return back and should ideally come to rest near x = 4.5 meters (x/L = 0.3).

7 DESCRIPTION OF THE NEW TEST FACILITY T3F.

7.1 Facility hardware

Figure 12 shows the set-up of the final test facility that consists of the pneumatic launcher, the railway tunnel model and the train model recovery. Most of the details have been discussed in chapter 5. A new detail is the provision to eliminate the jet from the launch tube that may precede the train model, see section 5.2.

To this end, the launch tube exit is closed with a plastic foil. This foil remains intact until it is penetrated by the nose of the train. To avoid any pressure above atmospheric that might cause premature bursting of the foil, the launch tube is partly evacuated before the actual launch of the train model. In addition, a dump tank is added. This tank is in open connection to the end of the launch tube and serves as escape reservoir for the air that is pushed forward by the train model towards the end of the launch tube.

Figures 13 and 14 show the train model approaching the tunnel entrance. The train model has a standard length of 2.3 meters. Visible are the contoured nose with the guidance ring and the guidance wires. The tunnel model is of the double track type in this case. Ahead of the tunnel entrance a photo-electric cell array is visible that is used for the measurement of the train velocity.

After its passage through the tunnel the train model is decelerated between two layers of foam rubber. About two meters are sufficient to bring the model to a full stop, requiring a deceleration of 500 g. Usually the model remains intact and can be re-used.

7.2 Data-acquisition and presentation

Figure 15 shows a diagram of the data-processing. The pressure transducers (piezo resistive) are mounted in the tunnel wall. Their range is 13.8 kPa differential pressure and their resonance frequency is about 70 kHz. The transducers are connected to a multi-channel conditioning unit (MCCU). The amplified pressure signals are fed to the measurement system (Leuven Measurements and Systems, with LMS-DIFA front-end), where they are filtered and digitalized (sampling frequency 20 kHz, 12 bit ADC). The signals of the photo-electric cells at the tunnel entrance and exit are also fed to the measurement system. The system is triggered by a signal from an accelerometer on the launching tube. With the present system up to 19 pressures can be measured and recorded simultaneously (using an other front-end a number of about 60 pressures is possible). The measured pressure histories can be presented immediately after the test.

A post processing system is available that predicts the pressure variations on the train itself, using the measured pressures on the tunnel wall. This processing is based on the assumption, that the pressure on the wall of the train equals the pressure on the opposite tunnel wall. Taking a certain point on the train model, its local pressure is known at each instant, that this point passes a tunnel wall pressure transducer. So, in case of 10 pressure transducers on the tunnel wall, the pressure on the train is known at 10 points in time. In between an interpolation procedure must be applied. This procedure is now standard and is applied when different pressure reducing measures are to be compared on the bases of passenger comfort.

7.3 Measurement accuracy and repeatability

The accuracy of the pressure measurements is about 35 Pa. The train velocity is determined with an accuracy of 0.1 m/s. It was found that between the tunnel entrance and exit the train velocity typically decreases by 3 percent in a 7.6 meter long tunnel model. It is estimated That a substantial part (but not the main part) of the train deceleration can then be attributed to friction on the wires.

To compare different tunnel configurations or pressure attenuating measures, data must be compared on the same basis, i.e. the train velocity. It has been demonstrated that three launches are usually sufficient to attain a train model velocity that differs less than 1 percent from its nominal value. This difference leads to a pressure deviation of 2 percent from the nominal value.

8 SOME TYPICAL TEST RESULTS

In this section some results are presented, that were obtained with the T3F prior to the actual test programm for HSL. The tests were performed in order to familiarise with the new facility and to explore its performance limits. The presented results were obtained using a blockage ratio of 13.5 percent.

Figure 16 shows a typical pressure history obtained with the reference train model (mass 0.13 kg, length 2.3 m) at a velocity of 83 m/s. The pressure is measured at mid tunnel position. Figure 17 shows the corresponding wave diagram. The principles of the wave diagram were explained in section 2. In both figures the compression, expansion waves and train passage are indicated with Roman numerals.

Figure 18 shows a comparison with theoretical calculations, performed by Vardy under contract with HSL. The time axis of the measurement was scaled upwards to real values. Very good agreement is found even in fine details. One exception is the pressure rise after the arrival of the first compression wave. This pressure rise is the result of the increasing aerodynamic blockage (displacement thickness) when the train is entering the tunnel (see also section 2).

The aerodynamic blockage is stronger with decreasing Reynolds number and increasing roughness of the train. To correct for these effects experimentally, the train model may be tapered towards the tail. In this way the solid plus aerodynamic blockage distribution of the real train can in principle be duplicated for the small scale experiment. Figure 19 shows the comparison of a such tapered train and the theoretical calculations of Vardy, that were shown in figure 18. The tapered train had an area reduction of 20 percent of the value at the nose. The maximum pressure in the tunnel (just before the drop caused by the expansion wave) has decreased with 13.5 percent.

Figure 20 shows the pressure measured at mid tunnel position for the reference train at three different velocities. The velocities are typical for a conventional train at 120 km/hr, a high speed train at 300 km/hr and an ultra high speed train at 500 km/hr. After the train has left the tunnel compression and expansion waves persist in the tunnel and die out due to viscous effects. Figure 18 clearly illustrates this. In real time these fluctuations will persist for a few minutes.

9 CONCLUDING REMARKS

The new train tunnel test facility T3F at NLR is a useful tool to determine the effect of measures to reduce the pressure variations in train tunnels.

The high validity of the test data has been demonstrated by comparison with theoretical predictions based on a one-dimensional flow model of Vardy.

The test facility will be extremely useful for situations where three-dimensional effects have to be taken into account or where the validity of a one-dimensional approach has to be demonstrated.

10 ACKNOWLEDGEMENT

NS Railinfrabeheer is gratefully acknowledged for their support to realise this facility and for their disposal of the theoretical results used in this paper.

Also a special word of thanks must be given to the colleagues at NLR that have contributed to the realization of the test facility.

REFERENCES

1. Vardy, A.E.; Aerodynamic Drag on Trains in Tunnels, Part 2: Prediction and Validation, Proceedings Institute of Mechanical Engineers Vol 210, Part F: Journal of Rail and Rapid Transit, 1996, pp. 39 - 49.
2. Sellmann, M.; Experimentelle und theoretische Bestimmung der Druckänderungen beim Entritt eines Hochgeswindigkeitstransportsystems in einen Tunnel, Dissertation, Technische Hochschule Darmstadt, 1978.
3. Dayman, B. and Vardy, A.E.; "TRUNNEL, A Gun-Fired 0.5 % Scale Facility for Pressure Transients of Very High Speed Trains in Tunnels", Proceedings of the 7th International Symposium on Aerodynamics and Ventilation of Vehicle Tunnels, Brighton 1991, Elsevier, pp. 757-787.
4. Takayama, K.; Sasoh, A.; Onodera, O.; Kaneko, R.; Matsui, Y.; Experimental Investigation on Tunnel Sonic Boom, Shock Waves 1995 (5), Springer Verlag, pp. e 127-138
5. Kazuyasu Matsuo; Toshiki Aoki; Hideo Kashimura; Mitsuru Kawaguchi; Nobutaka Takechi; Attenuation of Compression Waves in a High-Speed Railway Tunnelsimulator, Proceedings of the 7th International Symposium on Aerodynamics and Ventilation of Vehicle Tunnels, Brighton 1991, Elsevier, pp. 757-787.
6. Pope, C.W.; The Simulations of Flows in Railway Tunnels Using a $1/25^{th}$ scale moving facility, Proceedings of the 7th International Symposium on Aerodynamics and Ventilation of Vehicle Tunnels, Brighton 1991, Elsevier, pp. 709-737.

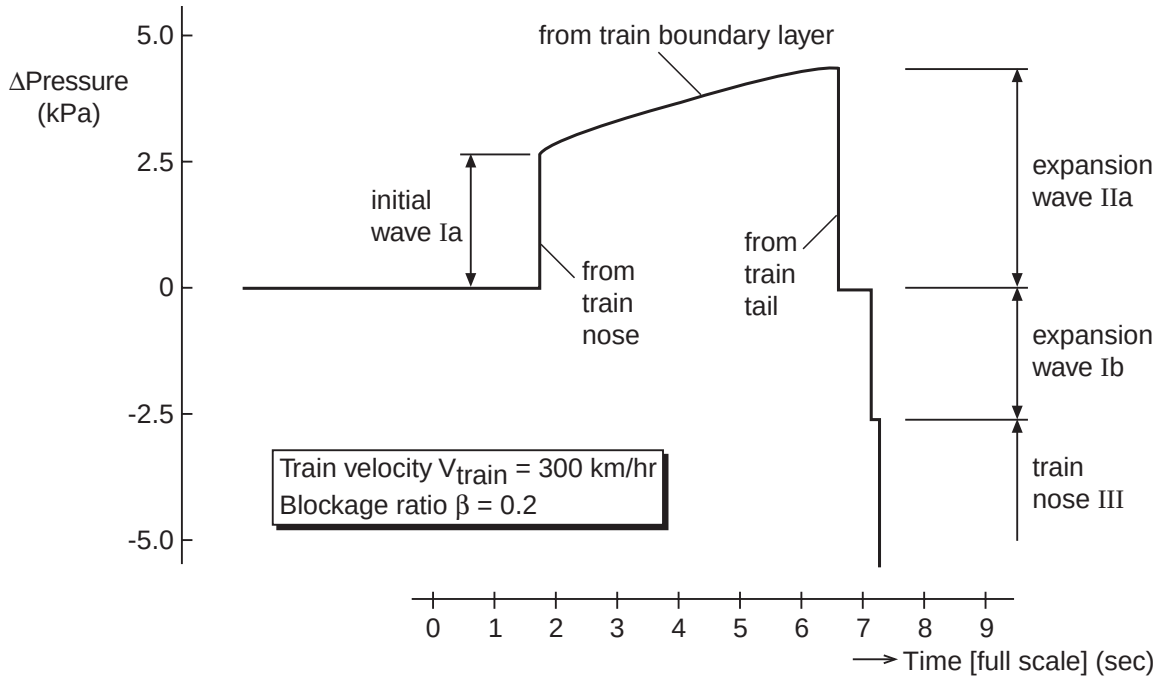

Fig. 2 Expected pressure history at x_2, see figure 1

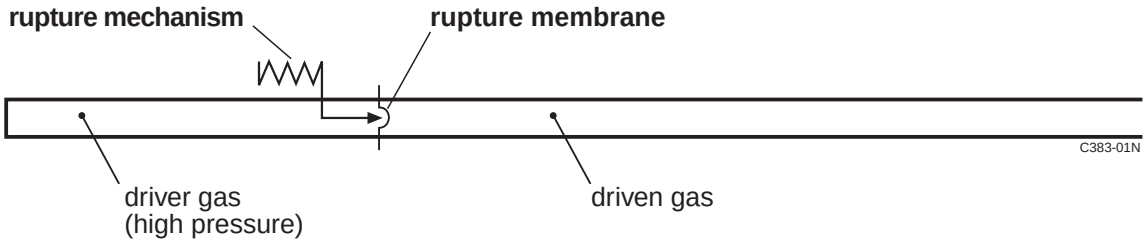

Fig. 3 Shock tube principle

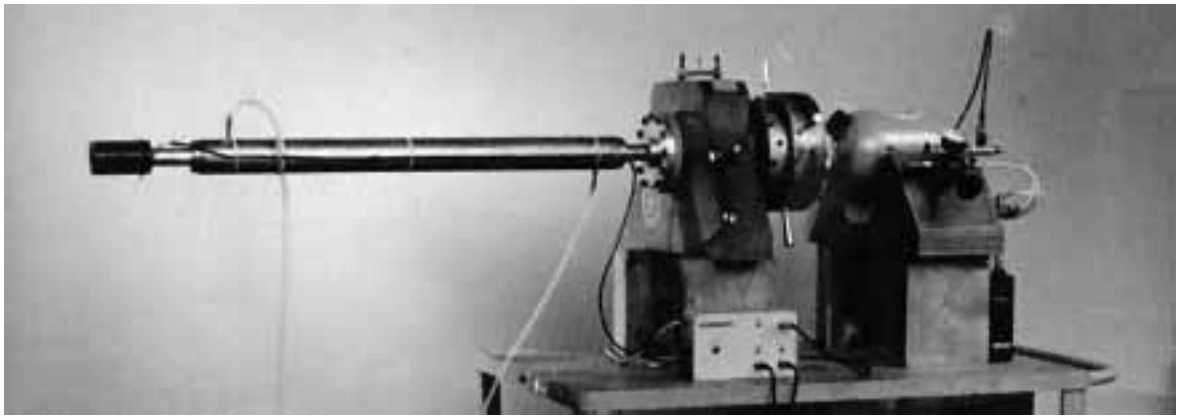

Fig. 4 The pneumatic projectile launcher used in the exploratory tests

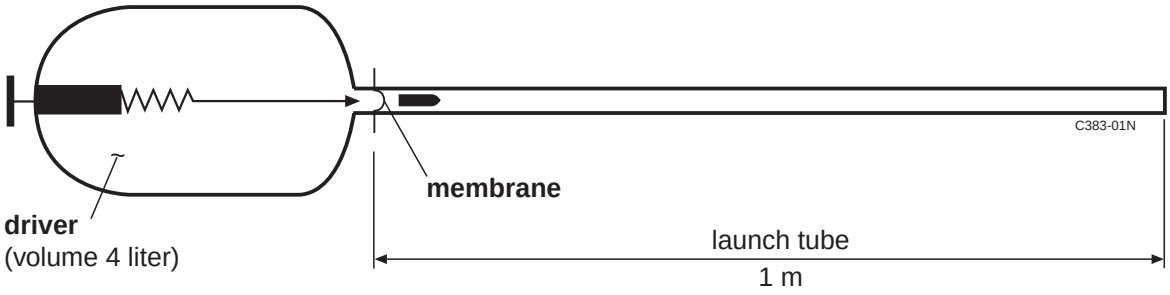

Fig. 5 Some technical details of the projectile launcher of figure 4

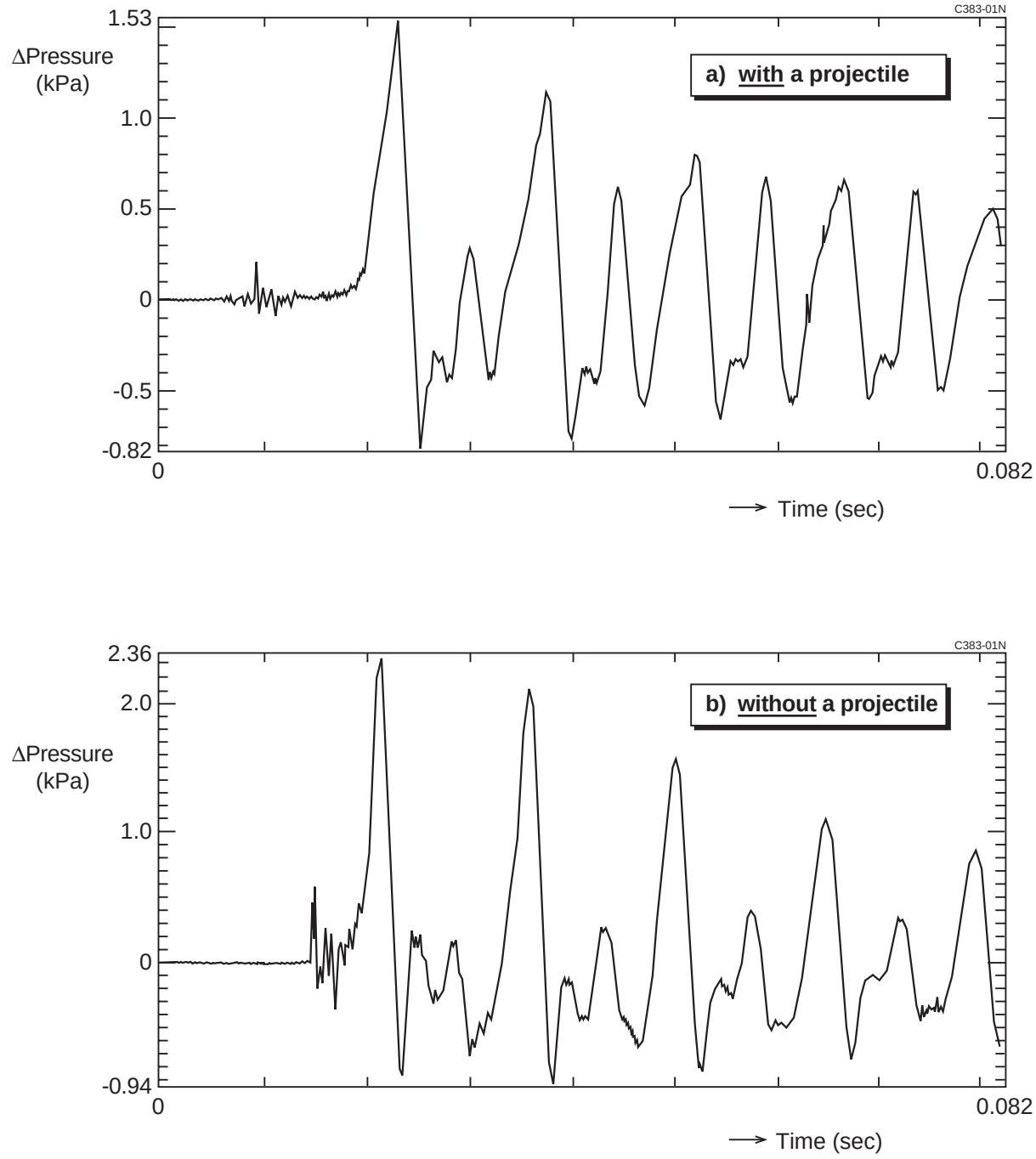

Fig. 6 Pressure trace measured in a first provisional tunnel model of a shot with and without a projectile using the facility of figure 4 (before modifications)

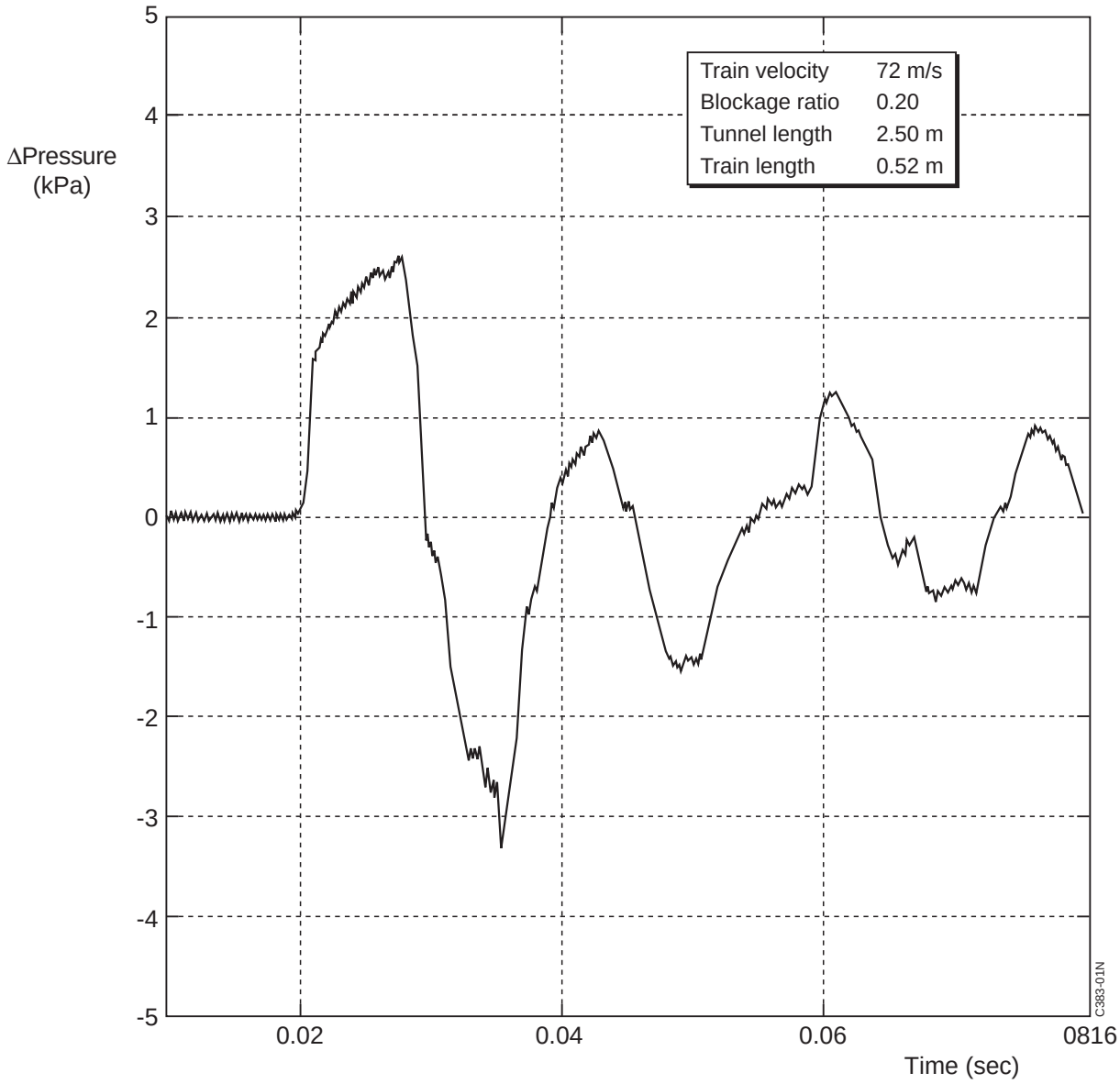

Fig. 7 A recorded pressure history in a second provisional tunnel model (at mid-tunnel position) after the modifications on the projectile launcher

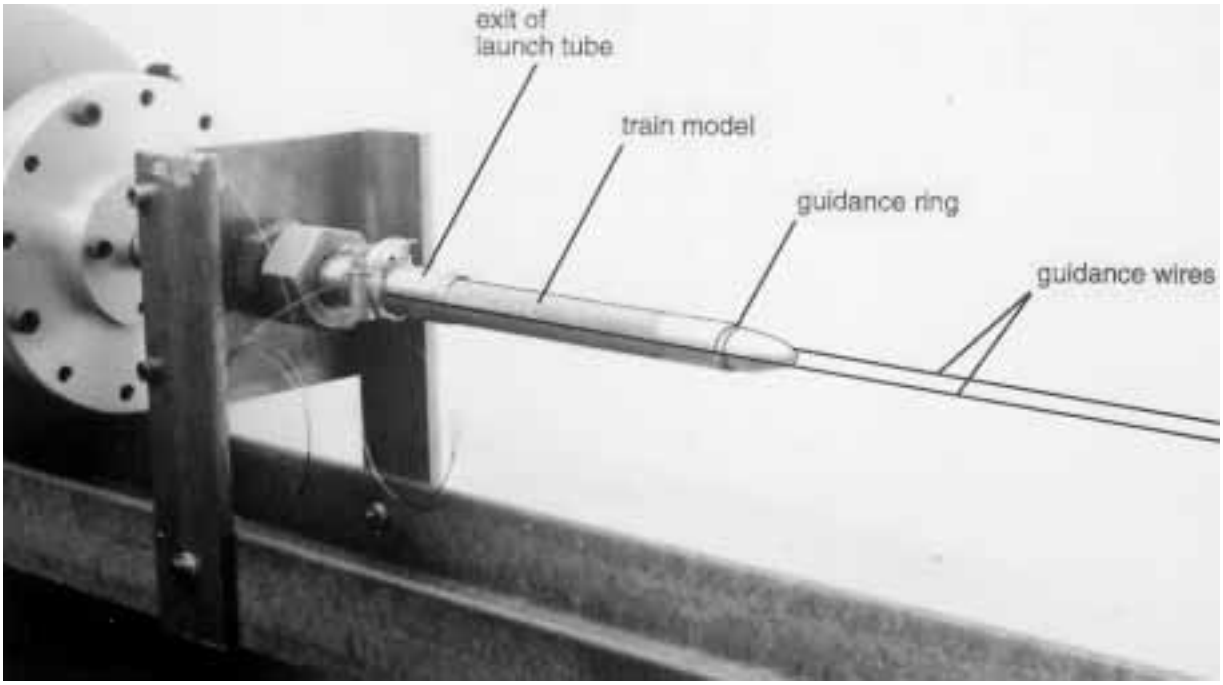

Fig. 8 Train model guidance

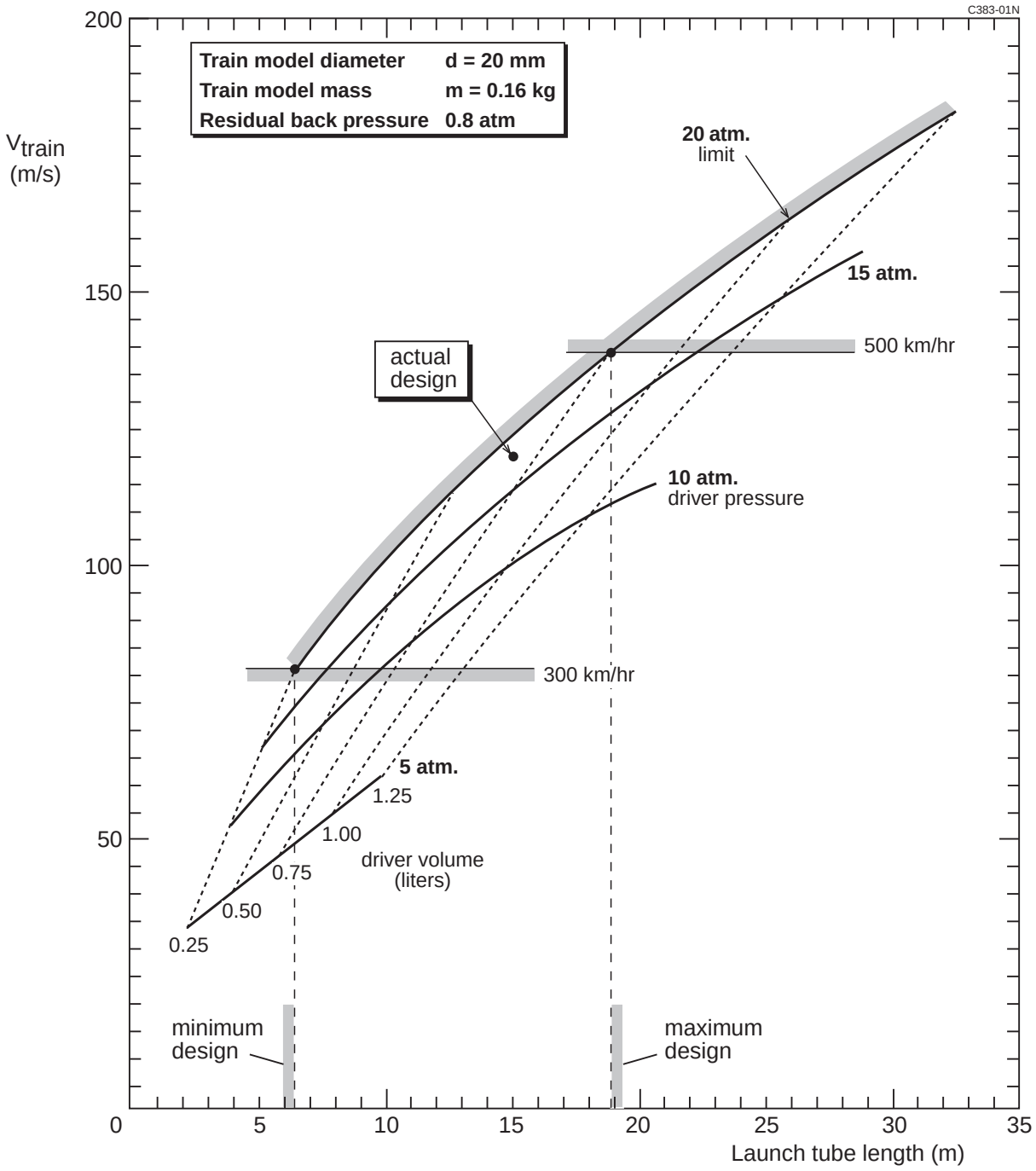

Fig. 9 Selection of launch tube length and driver volume for T3F

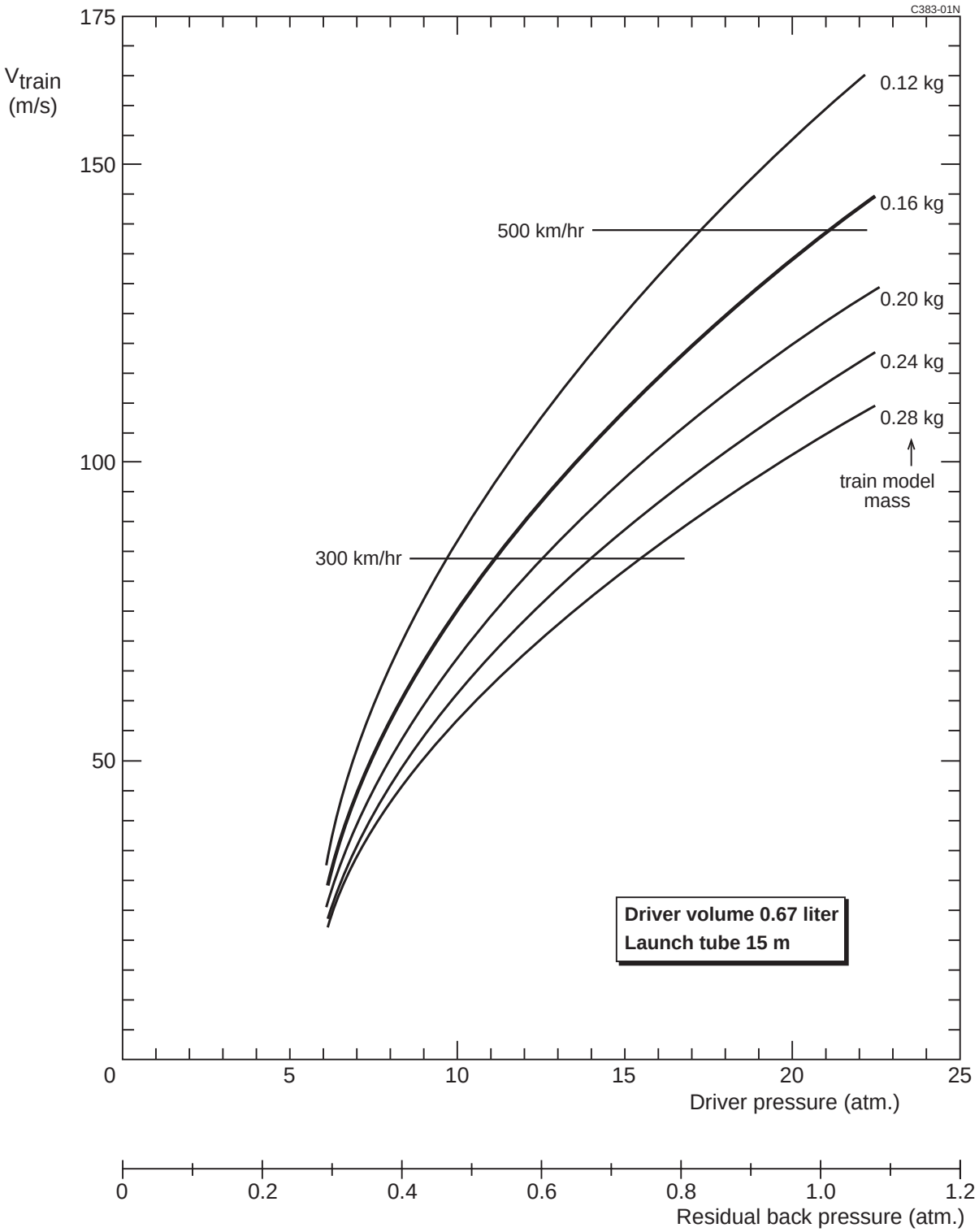

Fig. 10 Performance prediction of T3F

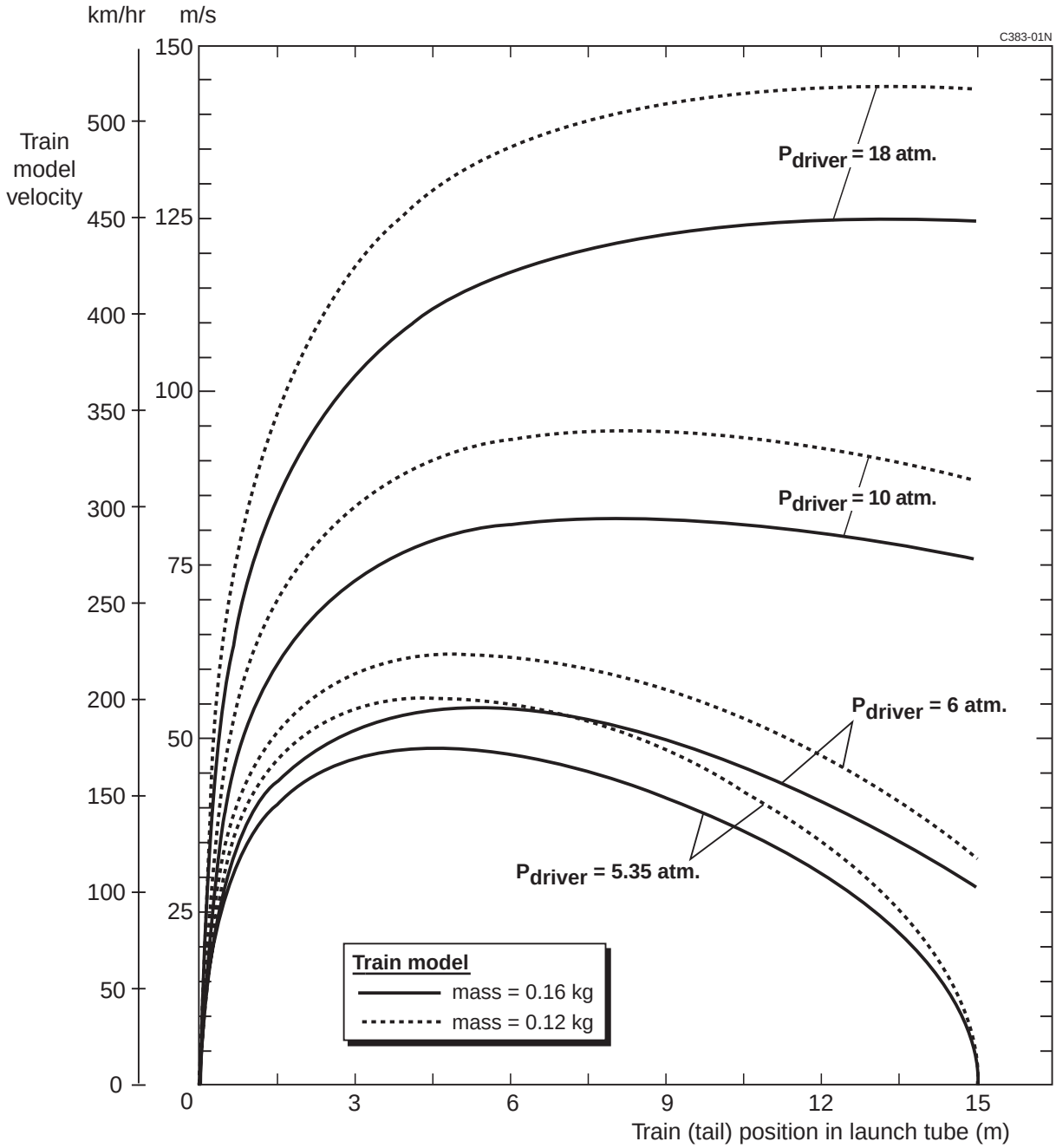

Fig. 11 Velocity of (the tail of) the train model in the launch tube at various driver pressures

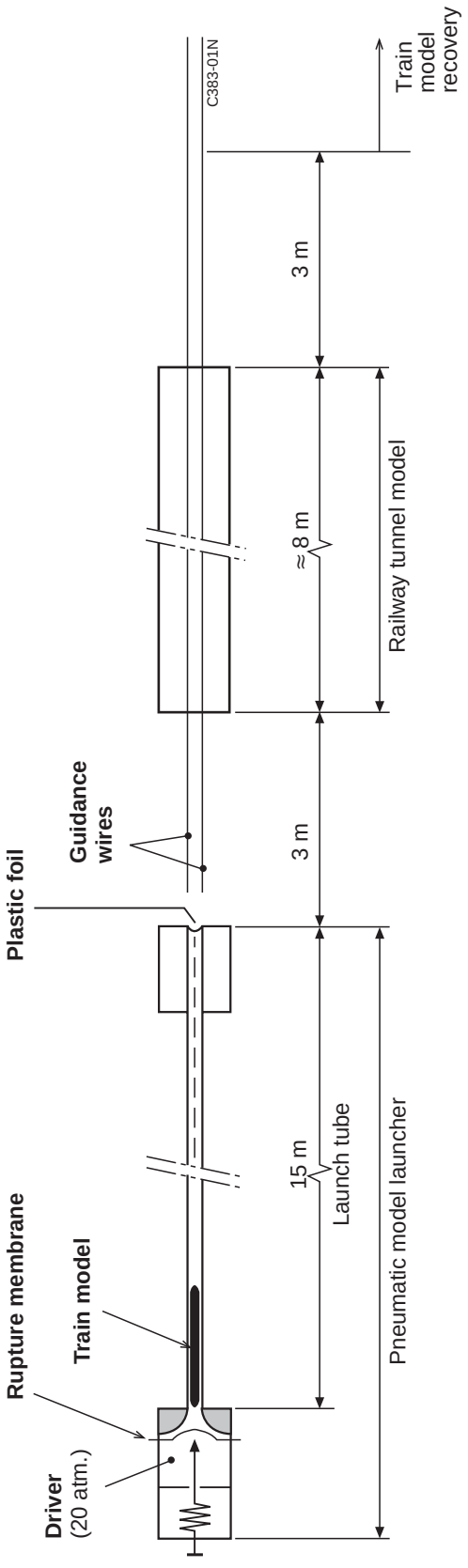

Fig. 12 Set up of T3F

Fig. 13 Train model at tunnel entrance (overview)

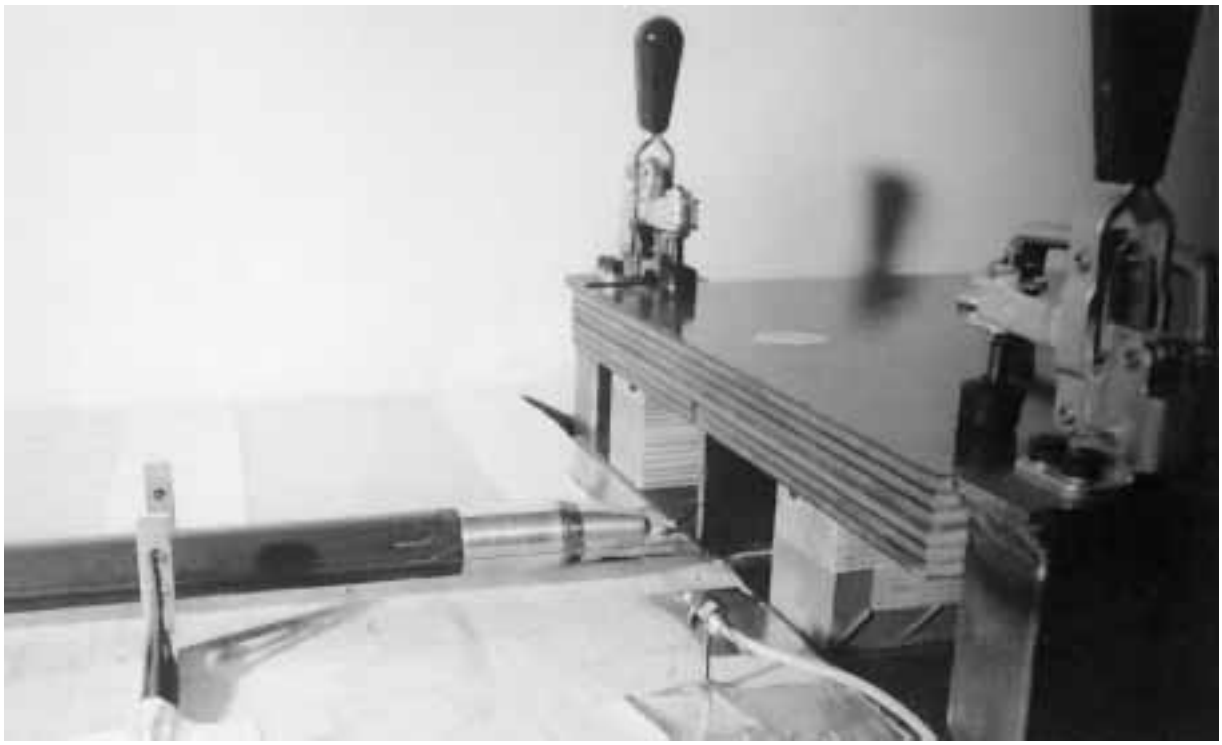

**Fig. 14 Train model entering the railway tunnel model.
On the left the photo-electric cell-array**

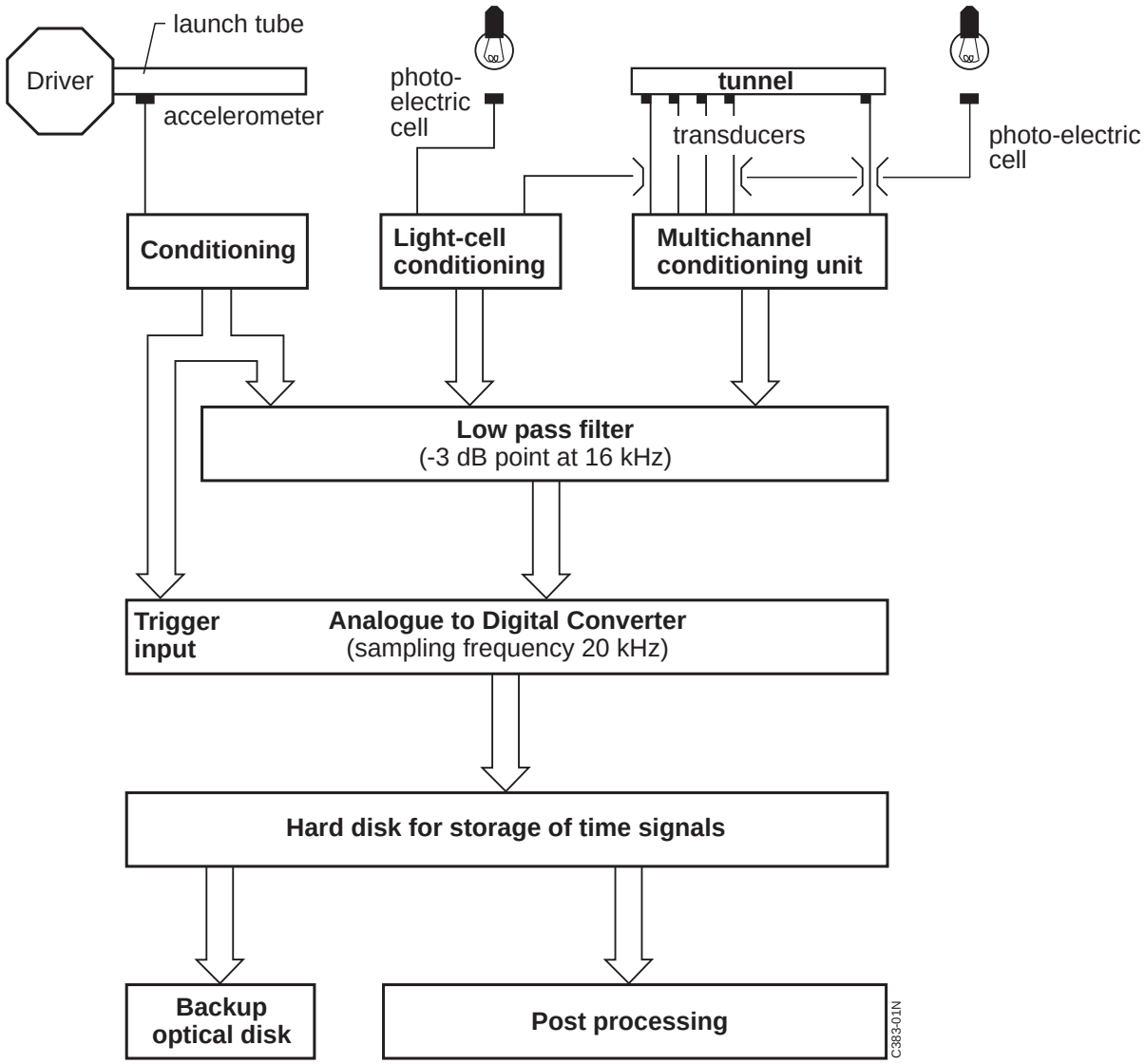

Fig. 15 Diagram of the data-acquisition

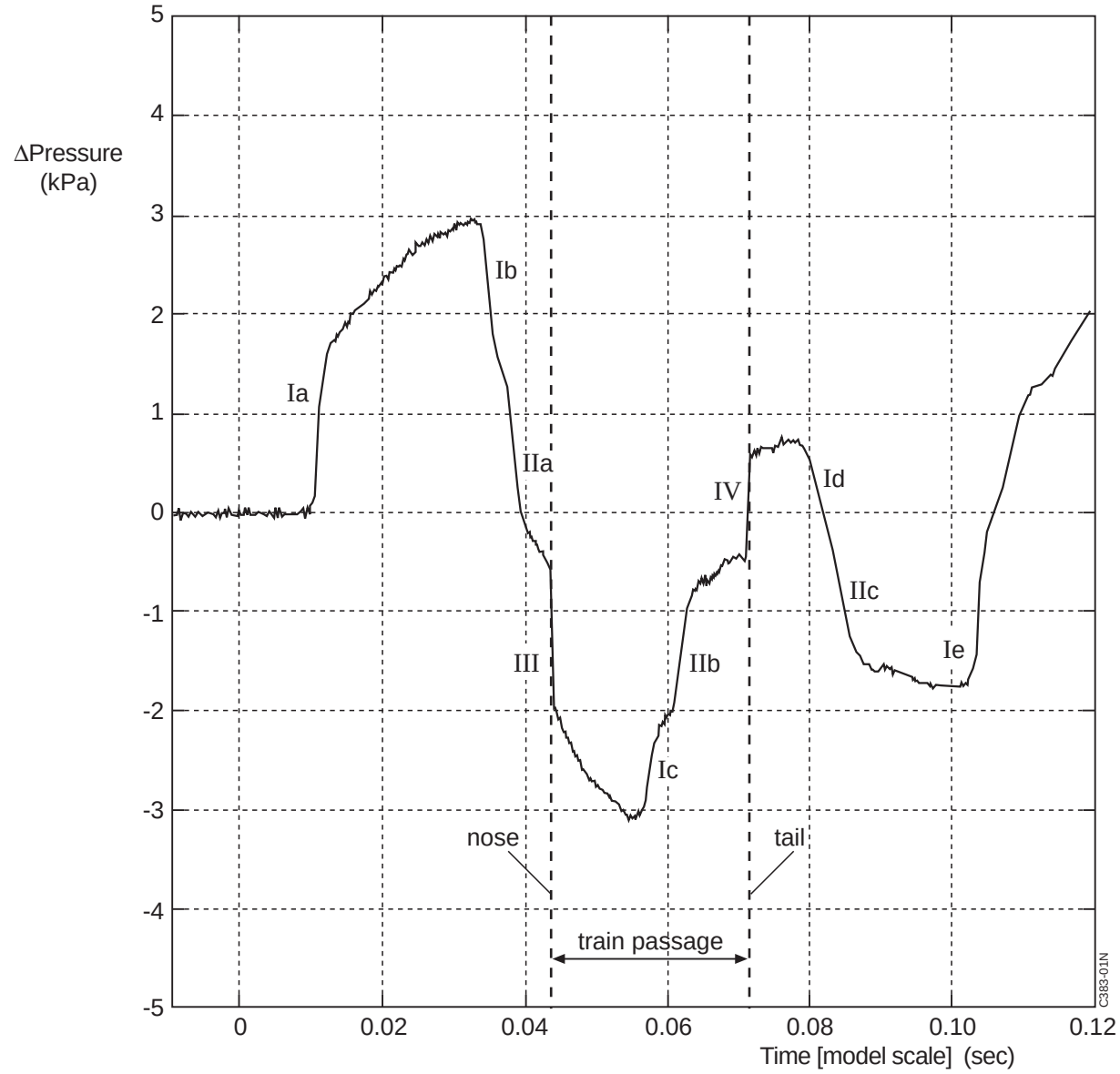

Fig. 16 Typical pressure history at mid tunnel position, see also figure 17 (V_{train} = 300 km/hr, β = 0.135)

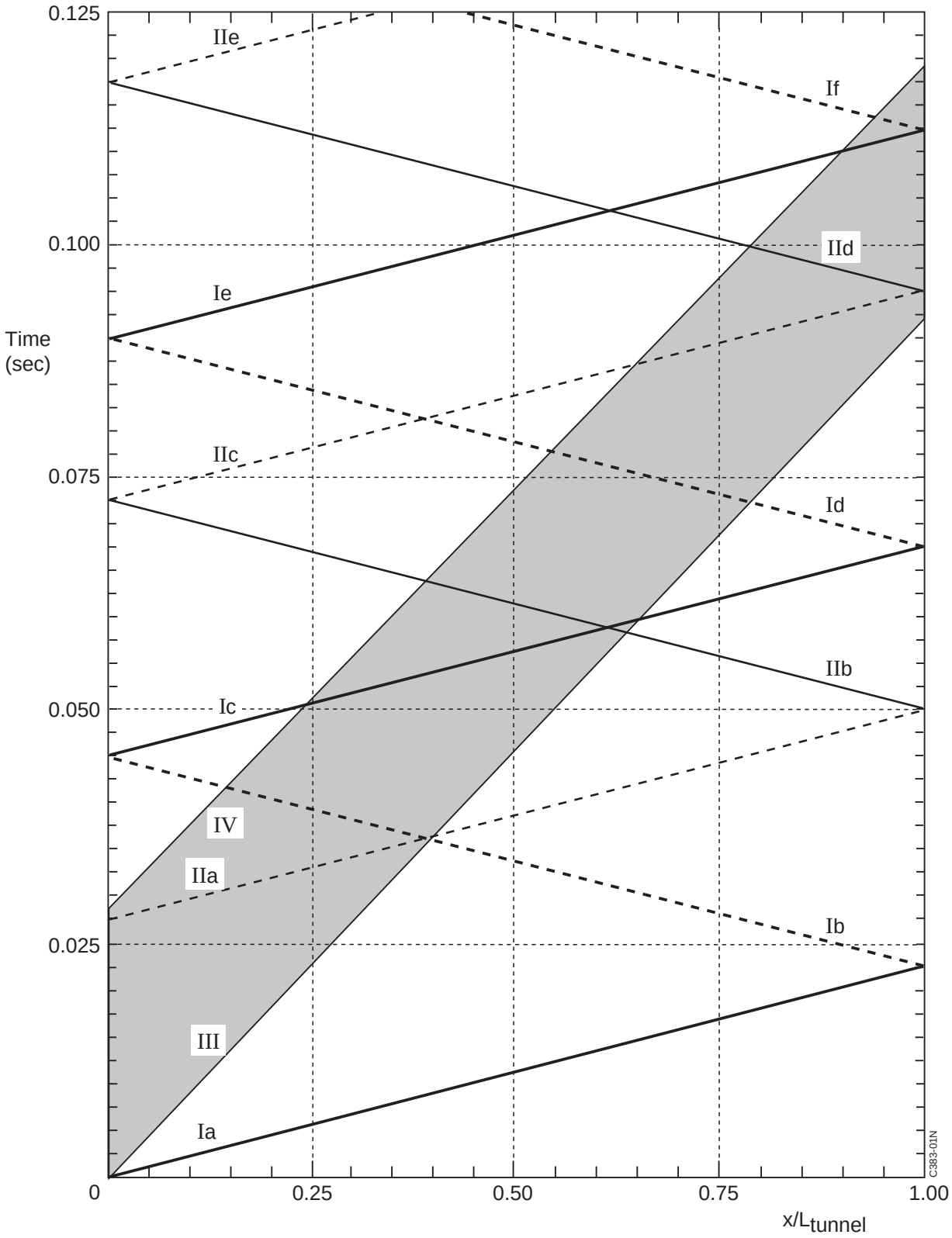

Fig. 17 Wave diagram corresponding to figure 16
(L_{tunnel} = 7.64 m, L_{train} = 2.3 m, V_{train} = 300 km/hr)

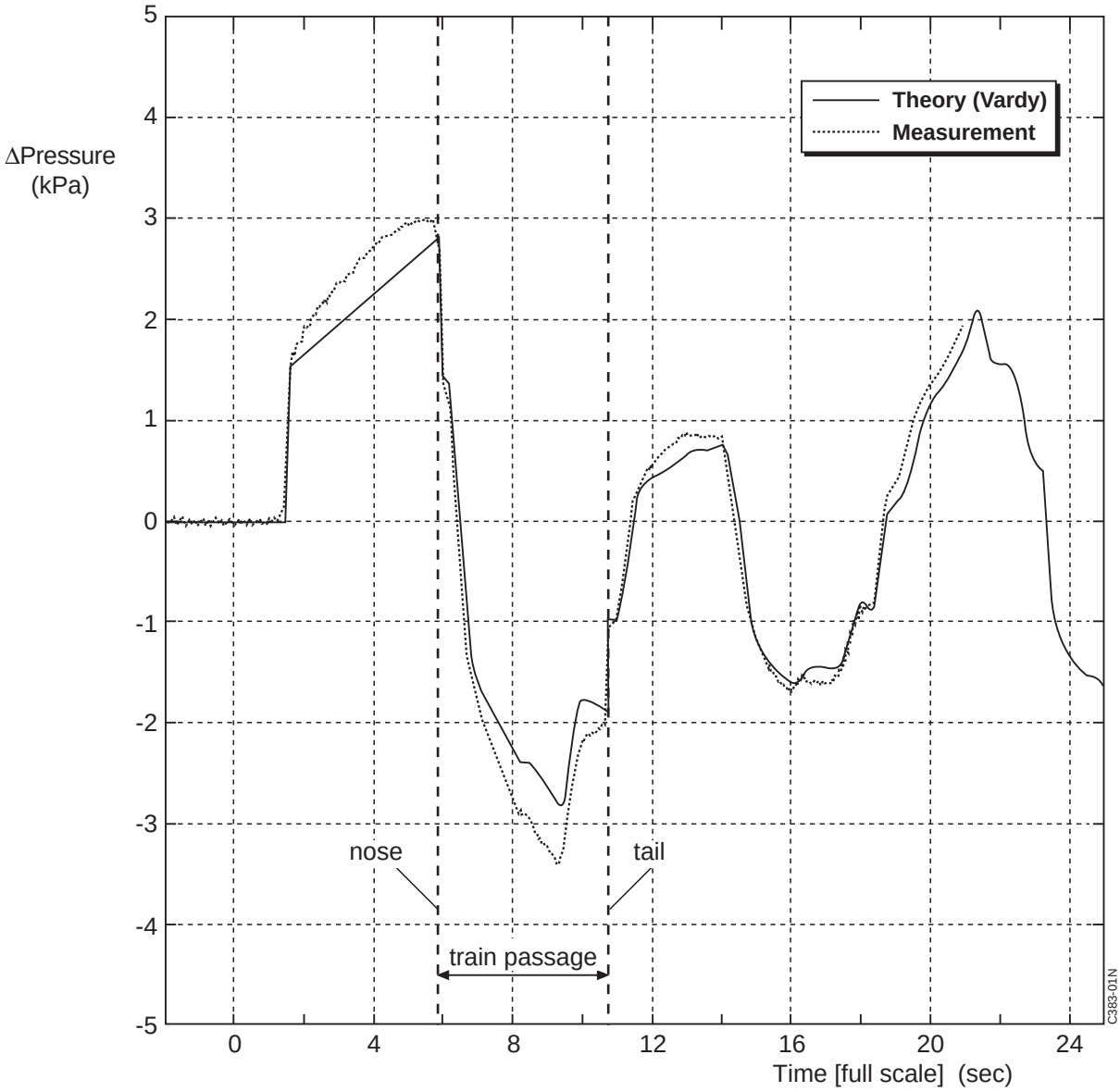

Fig. 18 Measured and calculated (Vardy) pressure history (x/L_{tunnel} = 0.38, β = 0.135, V_{train} = 300 km/hr)

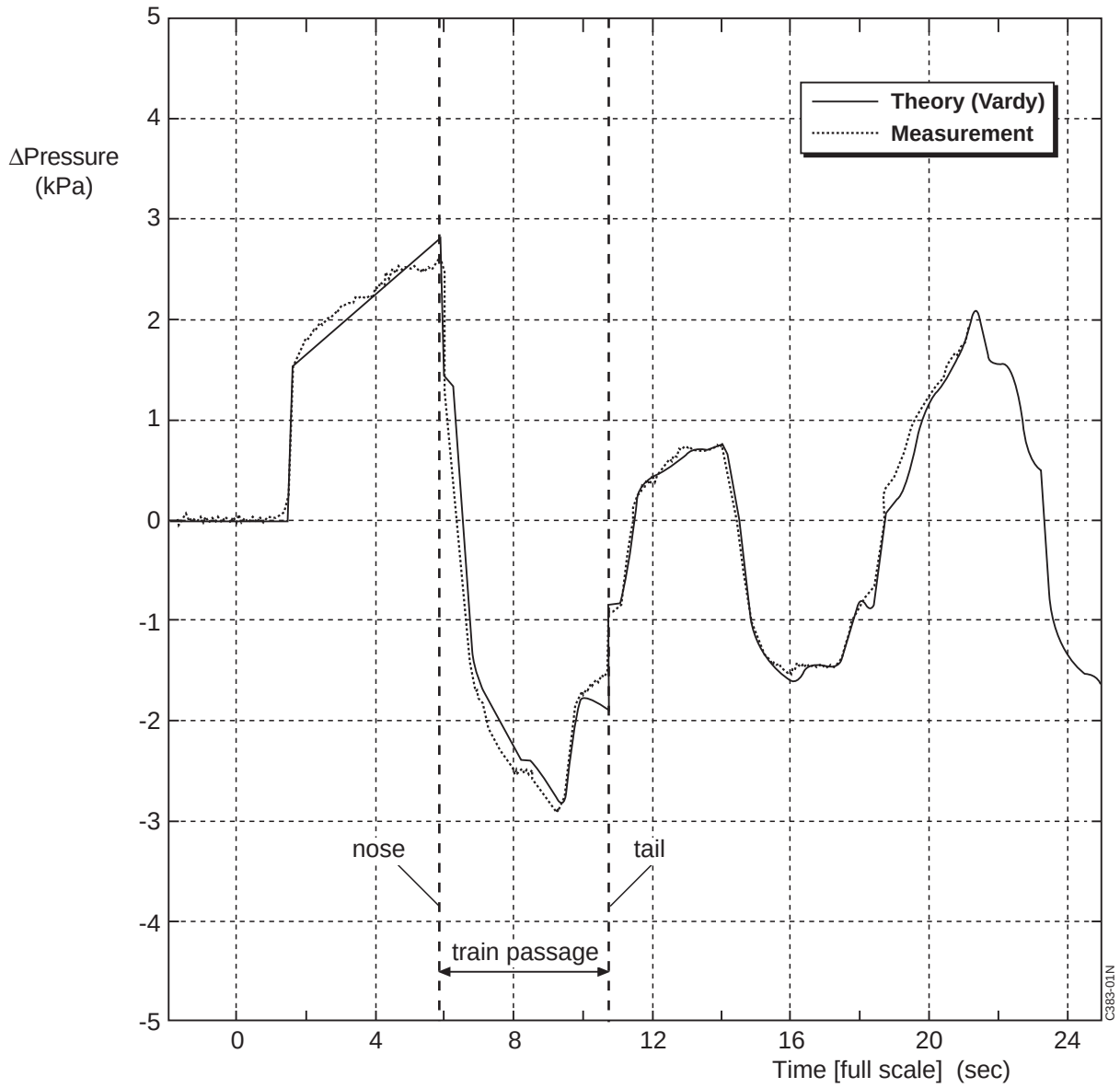

Fig. 19 Comparison between a calculated (Vardy) pressure history and a measured pressure history, using a tapered train model (conditions as in figure 18)

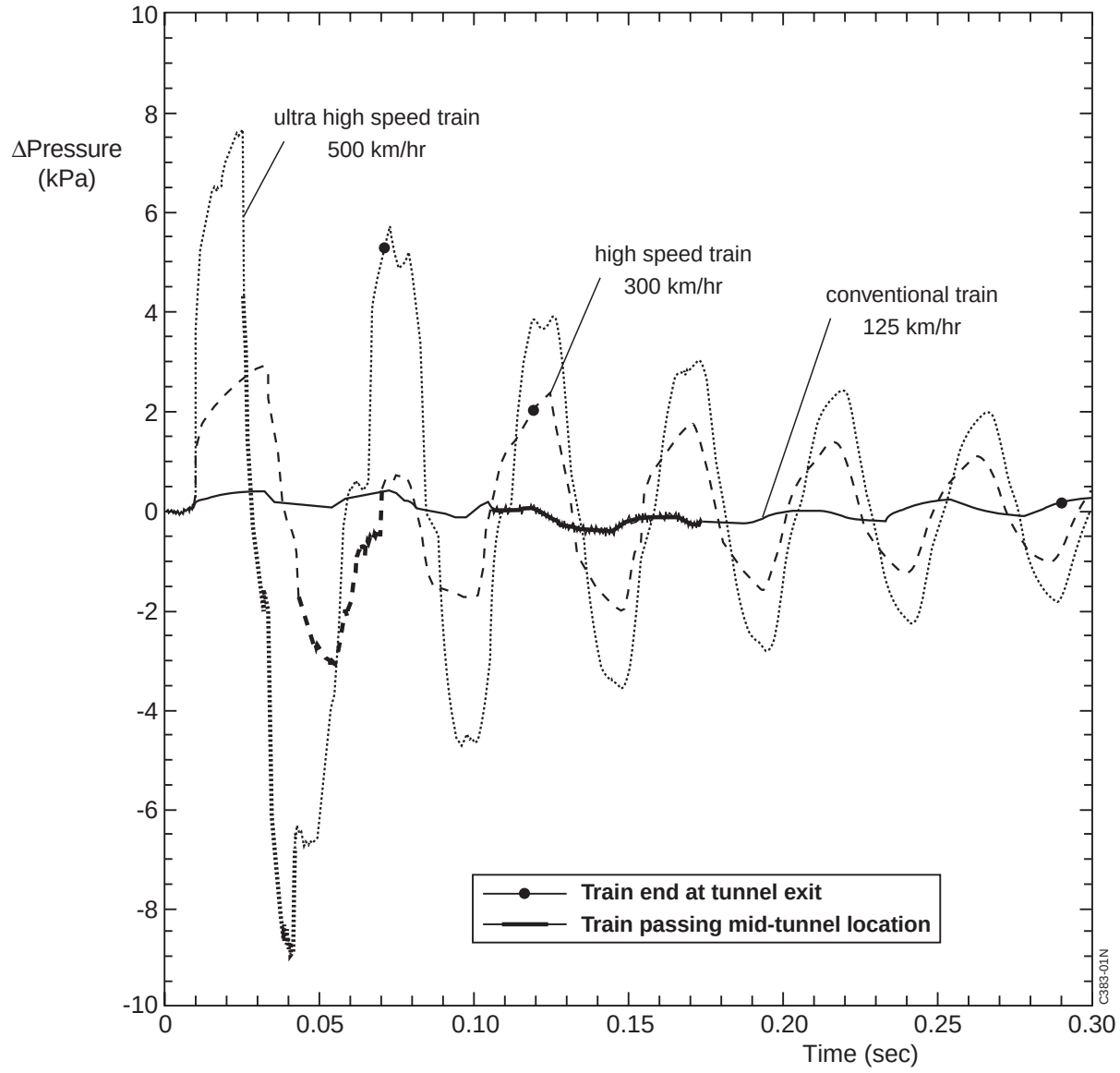

Fig. 20 Measured pressure histories at mid-tunnel position for the reference train at three velocities